Radial Basis Functions collocation for the bending and free vibration analysis of laminated plates using the Reissner-Mixed Variational Theorem.

Radial Basis Functions Collocation for the Bending and Free Vibration analysis of Laminated Plates using the Reissner-Mixed Variational Theorem

A.J.M. Ferreira, E. Carrera, M. Cinefra, C.M.C. Roque

PII: S0997-7538(12)00139-8

DOI: 10.1016/j.euromechsol.2012.10.012

Reference: EJMSOL 2878

To appear in: *European Journal of Mechanics / A Solids*

Received Date: 10 April 2012

Accepted Date: 30 October 2012

Please cite this article as: Ferreira, A.J.M., Carrera, E., Cinefra, M., Roque, C.M.C., Radial Basis Functions Collocation for the Bending and Free Vibration analysis of Laminated Plates using the Reissner-Mixed Variational Theorem, *European Journal of Mechanics / A Solids* (2012), doi: 10.1016/j.euromechsol.2012.10.012.

Highlights

- New meshless formulation with a Mixed formulation, including both displacements and stresses
- Radial basis function collocation of the Reissner-Mixed Variational Theorem
- Excellent results for static deformations and free vibrations of laminated plates

Radial Basis Functions Collocation for the Bending and Free Vibration analysis of Laminated Plates using the Reissner-Mixed Variational Theorem

A. J. M. Ferreira [a], E. Carrera [c], M. Cinefra [c], C. M. C. Roque [b],

[a] *Departamento de Engenharia Mecânica, Faculdade de Engenharia da Universidade do Porto, Rua Dr. Roberto Frias, 4200-465 Porto, Portugal*

[b] *INEGI, Faculdade de Engenharia da Universidade do Porto,Rua Dr. Roberto Frias, 4200-465 Porto, Portugal*

[c] *Departament of Aeronautics and Aerospace Engineering, Politecnico di Torino, Corso Duca degli Abruzzi, 24, 10129 Torino, Italy*

Abstract

In this paper, we combine the Carrera's Unified Formulation CUF (*E. Carrera. Theories and Finite elements for multilayered plates and shells: A unified compact formulation with numerical assessment and benchmarking. Arch. Comput. Meth. Eng., 10:215-297, 2003*) and a radial basis function (RBF) collocation technique for predicting the static deformations and free vibrations behavior of thin and thick cross-ply laminated plates. For the first time, the Reissner-Mixed Variational Theorem is used together with the RBF collocation to achieve a highly accurate technique. The accuracy and efficiency of this collocation technique for static and vibration problems are demonstrated through numerical examples.

1 Introduction

Multilayered structures are nowadays typical in airplanes, automobiles, aerospace applications, and so on. Examples of multilayered, anisotropic plate and shell structures are sandwich constructions, composite structures formed by stacking orthotropic laminae, as well as smart structures embedding piezo-layers.

The analysis of multilayered plates is more difficult than that of isotropic plates. Some three-dimensional analytical solutions have been presented [1–5]. Unfortunately these elasticity solutions are typically restricted to simple geometries, loadings and boundary conditions as well as material characteristics.

Two-dimensional analysis of layered structures also presents some difficulties, related to the discontinuity of the mechanical properties at each layer–interface that may produce high shear and normal transverse strains. Recent theories for the analysis of laminated plates are able to describe the so–called Zig-Zag (ZZ) [1] form of displacement fields in the thickness z–direction, as well as the inter-laminar continuous transverse shear and normal stresses (see [6–8] for detailed discussion).

A recent development by Carrera has found that many theories can be developed and implemented by various techniques in an automatic way by defining only the displacement expansion. This automatic technique was called Unified Formulation [6–8], and can be implemented in weak-form methods, such as the finite element method [9], or more recently in meshless methods based upon collocation with radial basis functions [10–14]. The use of alternative methods to the Finite Element Methods for the analysis of plates, such as the meshless methods based on radial basis functions is atractive due to the absence of a mesh and the ease of collocation methods. The use of radial basis function for the analysis of structures and materials has been previously studied by numerous authors [15–28]. Other alternative techniques based on weak-form approaches have been recently proposed in [29–32]. The use of weak-form based methods for the analysis with RMVT approach will be dealt in another paper.The unsymmetrical collocation technique developed by Kansa [33] was applied recently by the authors to the static deformations of composite beams and plates [34–36]. In [14] the Unified Formulation has been combined with radial basis functions to the analysis of thick laminated plates.

The Unified Formulation (here referred as CUF-Carrera's Unified Formulation) may consider both equivalent single layer theories (ESL), or layerwise theories (LW), using the Principle of Virtual Displacements (PVD). However, a more interesting (at a higher computational cost) approach is to use the layerwise formulation with the Reissner's Variational Mixed Theorem (RMVT). The RMVT considers two independent fields for displacement and transverse stress variables. As a result, a priori interlaminar continuous transverse shear and normal stress fields can be achieved, which is quite important for sandwich-like structures. Details on the RMVT can be found in Carrera [37,8,7]. This approach intends to improve existing shear deformation theories of first-order [38,39], or higher-order [40–44] to include Zig-zag effects and Interlaminar Continuity [2]. The ZZ and IC requirements (denoted by Car-

[1] Transverse discontinuous mechanical properties affect the displacement fields $\boldsymbol{u} = (u_1, u_2, u_3)$ in the thickness direction with rapid changes and different slopes in correspondence to each layer interface. This is known as the Zig-Zag, (ZZ) form of displacement fields in the thickness plate/shell direction.

[2] Although in-plane stresses $\boldsymbol{\sigma}_p$=$(\sigma_{11}, \sigma_{22}, \sigma_{12})$ can in general be discontinuous, equilibrium reasons i.e. the Cauchy theorem, demand continuous transverse stresses $\boldsymbol{\sigma}_n$=$(\sigma_{13}, \sigma_{23}, \sigma_{33})$ at each layer interface. This is often referred to in literature as

rera as the C_z^0 requirements) are crucial in the two-dimenional modelling of laminated plates and shells.

The majority of existing shear deformation theories do not describe adequately the interlaminar continuous transverse stresses. Typically, a post-processing procedure is required to recover $\boldsymbol{\sigma}_n$ stresses, but can be avoided if some stress assumptions are made. In-plane and transverse stresses can be assumed in the framework of mixed variational principles (see Reddy 1984a, and Atluri, Tong and Murakawa 1983). The Reissner's Mixed Variational Theorem can be seen as a mixed principle for multilayered structures, by restricting the stress assumptions to transverse components. Murakami (1984, 1985, 1986) was the first to apply RMVT to multilayered structures by assuming two independent fields for displacement and transverse stresses variables. Toledano and Murakami (1987a, 1987b) showed that RMVT does not experience any particular difficulties when including transverse normal stresses in a plate theory. (Carrera 1998) showed that the RMVT leads to a quasi–3D description of the in-plane and out-of plane response. In particular, transverse stresses were determinate *a priori* with excellent accuracy. It can be concluded that RMVT appears to be a natural tool to completely and a priori fulfill the C_z^0–Requirements in both LW and ESL cases.

The RMVT has been implemented successfully with finite elements, but never with collocation with radial basis functions. Therefore, this paper serves to fill the gap of knowledge in this research area.

2 The radial basis function method

In this section the global unsymmetrical collocation RBF-based method in static and free vibration problems is discussed.

The radial basis function (ϕ) approximation of a function ($\mathbf{u}$) is given by

$$\widetilde{\mathbf{u}}(\mathbf{x}) = \sum_{i=1}^{N} \alpha_i \phi \left(\|x - y_i\|_2 \right), \mathbf{x} \in \mathbb{R}^n \tag{1}$$

where $y_i, i = 1, .., N$ is a finite set of distinct points (centers) in $\mathbb{R}^n$. Some of

Interlaminar Continuity, (IC) of transverse shear and normal stresses.

the most common RBFs are

$$\begin{aligned} \text{Wendland functions:} \quad & \phi(r) = (1-r)_+^m p(r) \\ \text{Gaussian:} \quad & \phi(r) = e^{-(cr)^2} \\ \text{Multiquadrics:} \quad & \phi(r) = \sqrt{c^2 + r^2} \\ \text{Inverse Multiquadrics:} \quad & \phi(r) = (c^2 + r^2)^{-1/2} \end{aligned}$$

where the Euclidian distance r is real and non-negative and c is a positive shape parameter. Following Kansa [33] method, we consider N distinct points. Taking $u(x_j), j = 1, 2, ..., N$, we find α_i by solving a $N \times N$ linear system

$$\mathbf{A}\boldsymbol{\alpha} = \mathbf{u} \tag{2}$$

where $\mathbf{A} = [\phi(\|x - y_i\|_2)]_{N\times N}$, $\boldsymbol{\alpha} = [\alpha_1, \alpha_2, ..., \alpha_N]^T$ and $\mathbf{u} = [u(x_1), u(x_2), ..., u(x_N)]^T$.

The solution of the static problem by radial basis functions considers N_I nodes in the domain and N_B nodes on the boundary, with a total number of nodes $N = N_I + N_B$. We denote the sampling points by $x_i \in \Omega, i = 1, ..., N_I$ and $x_i \in \partial\Omega, i = N_I + 1, ..., N$. At the points in the domain we solve the following system of equations

$$\sum_{i=1}^{N} \alpha_i \mathcal{L}\phi(\|x - y_i\|_2) = \mathbf{f}(x_j), j = 1, 2, ..., N_I \tag{3}$$

or

$$\mathcal{L}^I\boldsymbol{\alpha} = \mathbf{F} \tag{4}$$

where

$$\mathcal{L}^I = [\mathcal{L}\phi(\|x - y_i\|_2)]_{N_I\times N} \tag{5}$$

At the points on the boundary, we impose boundary conditions as

$$\sum_{i=1}^{N} \alpha_i \mathcal{L}_B\phi(\|x - y_i\|_2) = \mathbf{g}(x_j), j = N_I + 1, ..., N \tag{6}$$

or

$$\mathbf{B}\boldsymbol{\alpha} = \mathbf{G} \tag{7}$$

where

$$\mathbf{B} = \mathcal{L}_B\phi[(\|x_{N_I+1} - y_j\|_2)]_{N_B\times N}$$

Therefore, we can write a finite-dimensional static problem as

$$\begin{bmatrix} \mathcal{L}^I \\ \mathbf{B} \end{bmatrix} \boldsymbol{\alpha} = \begin{bmatrix} \mathbf{F} \\ \mathbf{G} \end{bmatrix} \tag{8}$$

By inverting the system (8), we obtain the vector $\boldsymbol{\alpha}$. We then obtain the solution $\mathbf{u}$ using the interpolation equation (1). We now compute

$$\boldsymbol{\alpha} = \begin{bmatrix} L^I \\ \mathbf{B} \end{bmatrix}^{-1} \begin{bmatrix} \mathbf{F} \\ \mathbf{G} \end{bmatrix} \tag{9}$$

This $\boldsymbol{\alpha}$ vector is then used to obtain solution $\tilde{\mathbf{u}}$, by using (1). If derivatives of $\tilde{\mathbf{u}}$ are needed, such derivatives are computed as

$$\frac{\partial \tilde{\mathbf{u}}}{\partial x} = \sum_{j=1}^{N} \alpha_j \frac{\partial \phi_j}{\partial x} \tag{10}$$

$$\frac{\partial^2 \tilde{\mathbf{u}}}{\partial x^2} = \sum_{j=1}^{N} \alpha_j \frac{\partial^2 \phi_j}{\partial x^2}, \text{etc} \tag{11}$$

In the present collocation approach, we need to impose essential and natural boundary conditions. Consider, for example, the condition $w = 0$, on a simply supported or clamped edge. We enforce the conditions by interpolating as

$$w = 0 \rightarrow \sum_{j=1}^{N} \alpha_j^W \phi_j = 0 \tag{12}$$

Other boundary conditions are interpolated in a similar way.

Taking into account the large number of degrees of freedom per node ($30 \times N$), where N is the total number of discretization points, the solution of the static problem follows a static condensation procedure as follows. Consider the global system of equations (after imposing boundary conditions):

$$\begin{bmatrix} \mathbf{K_{uu}} & \mathbf{K_{u\sigma}} \\ \mathbf{K_{\sigma u}} & \mathbf{K_{\sigma\sigma}} \end{bmatrix} \begin{bmatrix} \mathbf{u} \\ \boldsymbol{\sigma} \end{bmatrix} = \begin{bmatrix} \mathbf{f} \\ \mathbf{0} \end{bmatrix} \tag{13}$$

The problem is reduced to

$$\mathbf{K^*_{uu}} \mathbf{u} = \mathbf{f} \tag{14}$$

where $\mathbf{K^*}_{uu} = \mathbf{K}_{uu} - \mathbf{K}_{u\sigma}[\mathbf{K}_{\sigma\sigma}]^{-1}\mathbf{K}_{\sigma u}$. After computation of the solution, transverse stresses are readily computed at each interface by

$$\boldsymbol{\sigma} = [\mathbf{K}_{\sigma\sigma}]^{-1} \left(-\mathbf{K}_{\sigma \mathbf{u}} \mathbf{u}\right) \tag{15}$$

For the solution of free vibrations, at the points in the domain, we define the eigen-problem as

$$\sum_{i=1}^{N} \alpha_i \mathcal{L}\phi\left(\|x - y_i\|_2\right) = \lambda \tilde{\mathbf{u}}(x_j), j = 1, 2, ..., N_I \tag{16}$$

or

$$\mathcal{L}^I \boldsymbol{\alpha} = \lambda \tilde{\mathbf{u}}^I \tag{17}$$

where

$$\mathcal{L}^I = \left[\mathcal{L}\phi\left(\|x - y_i\|_2\right)\right]_{N_I \times N} \tag{18}$$

At the points on the boundary, we enforce the boundary conditions as

$$\sum_{i=1}^{N} \alpha_i \mathcal{L}_B\phi\left(\|x - y_i\|_2\right) = 0, j = N_I + 1, ..., N \tag{19}$$

or

$$\mathbf{B}\boldsymbol{\alpha} = 0 \tag{20}$$

Equations (17) and (20) can now be solved as a generalized eigenvalue problem

$$\begin{bmatrix} \mathcal{L}^I \\ \mathbf{B} \end{bmatrix} \boldsymbol{\alpha} = \lambda \begin{bmatrix} \mathbf{A}^I \\ \mathbf{0} \end{bmatrix} \boldsymbol{\alpha} \tag{21}$$

where

$$\mathbf{A}^I = \phi\left[\left(\|x_{N_I} - y_j\|_2\right)\right]_{N_I \times N} F_t F_s \rho^k$$

For free vibration problems we set the external force to zero, and assume harmonic solution in terms of displacements u^k, v^k, w^k, for each layer, as

$$u^k = U^k(w, y)e^{i\omega t}; \quad v^k = V^k(w, y)e^{i\omega t}; \quad w^k = W^k(w, y)e^{i\omega t} \tag{22}$$

where ω is the frequency of natural vibration. Substituting the harmonic expansion into equations (21) in terms of the amplitudes U^k, V^k, W^k, we may obtain the natural frequencies and vibration modes for the plate problem, by solving the eigenproblem

$$\left[\mathcal{L} - \omega^2 \mathcal{G}\right] \mathbf{X} = \mathbf{0} \tag{23}$$

where $\mathcal{L}$ collects all stiffness terms and $\mathcal{G}$ collects all terms related to the inertial terms. In (23) $\mathbf{X}$ are the modes of vibration associated with the natural frequencies defined as ω.

3 Governing equations by RMVT

The Reissner's Mixed Variational Theorem is obtained via the addition of a Lagrange's Multiplier that permits to modelling the transverse shear/normal stresses $\boldsymbol{\sigma_n}$:

$$\sum_{k=1}^{N_l} \int_{\Omega_k} \int_{A_k} \left\{ \delta {\boldsymbol{\epsilon}_{pG}^k}^T \boldsymbol{\sigma}_{pC}^k + \delta {\boldsymbol{\epsilon}_{nG}^k}^T \boldsymbol{\sigma}_{nM}^k + \delta {\boldsymbol{\sigma}_{nM}^k}^T (\boldsymbol{\epsilon}_{nG}^k - \boldsymbol{\epsilon}_{nC}^k) \right\} d\Omega_k dz = \sum_{k=1}^{N_l} \delta L_e^k \tag{24}$$

As above, subscripts G and C indicate geometrical and constitutive equations respectively, while M indicates that the variable is modelled because it is assumed "a priori".

The expressions of the constitutive relations for a classical model, opportunely separated in in-plane and out-plane components state:

$$\begin{aligned} \boldsymbol{\sigma}_p^k &= \boldsymbol{C}_{pp}^k(z)\, \boldsymbol{\epsilon}_p^k + \boldsymbol{C}_{pn}^k(z)\, \boldsymbol{\epsilon}_n^k \\ \boldsymbol{\sigma}_n^k &= \boldsymbol{C}_{np}^k(z)\, \boldsymbol{\epsilon}_p^k + \boldsymbol{C}_{nn}^k(z)\, \boldsymbol{\epsilon}_n^k \end{aligned} \tag{25}$$

In case of RMVT displacements $\boldsymbol{u}$ and transverse shear/normal stresses $\boldsymbol{\sigma_n}$ are both a priori variables, so constitutive equations are rewritten as:

$$\begin{aligned} \boldsymbol{\sigma}_p^k &= \tilde{\boldsymbol{C}}_{pp}^k(z)\, \boldsymbol{\epsilon}_p^k \; + \; \tilde{\boldsymbol{C}}_{pn}^k(z)\, \boldsymbol{\sigma}_n^k \\ \boldsymbol{\epsilon}_n^k &= \tilde{\boldsymbol{C}}_{np}^k(z)\, \boldsymbol{\epsilon}_p^k \; + \; \tilde{\boldsymbol{C}}_{nn}^k(z)\, \boldsymbol{\sigma}_n^k \end{aligned} \tag{26}$$

where the new coefficients are:

$$\begin{aligned} \tilde{\boldsymbol{C}}_{pp}^k(z) &= \boldsymbol{C}_{pp}^k(z) - \boldsymbol{C}_{pn}^k(z) \boldsymbol{C}_{nn}^{k^{-1}}(z) \boldsymbol{C}_{np}^k(z) & \tilde{\boldsymbol{C}}_{pn}^k(z) &= \boldsymbol{C}_{pn}^k(z) \boldsymbol{C}_{nn}^{k^{-1}}(z) \\ \tilde{\boldsymbol{C}}_{np}^k(z) &= -\boldsymbol{C}_{nn}^{k^{-1}}(z) \boldsymbol{C}_{np}(z) & \tilde{\boldsymbol{C}}_{nn}^k(z) &= \boldsymbol{C}_{nn}^{k^{-1}}(z) \end{aligned} \tag{27}$$

Layer Wise (LW) approach describes the layers as independent. This description can be applied to displacement components $\boldsymbol{u}$ and transverse shear/normal stresses $\boldsymbol{\sigma}_n = (\sigma_{xz}, \sigma_{yz}, \sigma_{zz})$. Stresses are always modelled via LW to ensure the interlaminar continuity, the displacements instead can be modelled ESL or LW. Layer Wise description is introduced according to the following expansion:

$$\boldsymbol{\sigma}_n^k = \; F_t\, \boldsymbol{\sigma}_{nt}^k \; + \; F_b\, \boldsymbol{\sigma}_{nb}^k \; + \; F_l\, \boldsymbol{\sigma}_{nl}^k = \; F_\tau\, \boldsymbol{\sigma}_\tau^k \tag{28}$$

where

$$\tau = t, b, l \quad with \quad l = 2, \ldots, N$$

We are using linear functions in each layer, as follows:

$$F_b = 0.5 - \frac{1}{h_k}\left(z - \frac{z_b(k) + z_t(k)}{2}\right); \quad F_t = 0.5 + \frac{1}{h_k}\left(z - \frac{z_b(k) + z_t(k)}{2}\right) \tag{29}$$

After substitution of the geometrical relations for the plate, the constitutive equations Eqs.(26) and the CUF for both displacement components and transverse stresses in Eq.(24) , and then performing the integration by parts, the governing equations in case of RMVT are:

$$\begin{aligned} \delta \boldsymbol{u}_s^{k\,T} : \quad & \boldsymbol{K}_{uu}^{k\tau s}\,\boldsymbol{u}_\tau^k + \boldsymbol{K}_{u\sigma}^{k\tau s}\,\boldsymbol{\sigma}_{n\tau}^k = \boldsymbol{P}_{u\tau}^k \\ \delta \boldsymbol{\sigma}_{ns}^{k\,T} : \quad & \boldsymbol{K}_{\sigma u}^{k\tau s}\,\boldsymbol{u}_\tau^k + \boldsymbol{K}_{\sigma\sigma}^{k\tau s}\,\boldsymbol{\sigma}_{n\tau}^k = 0 \end{aligned} \tag{30}$$

with boundary conditions state:

$$\boldsymbol{\Pi}_u^{k\tau s}\,\boldsymbol{u}_\tau^k + \boldsymbol{\Pi}_\sigma^{k\tau s}\,\boldsymbol{\sigma}_{n\tau}^k = \boldsymbol{\Pi}_u^{k\tau s}\,\bar{\boldsymbol{u}}_\tau^k + \boldsymbol{\Pi}_\sigma^{k\tau s}\,\bar{\boldsymbol{\sigma}}_{n\tau}^k \tag{31}$$

Note that we don't have boundary conditions for $\boldsymbol{\sigma}_n$.

The expression of fundamental nuclei is:

$$\boldsymbol{K}_{uu}^{k\tau s} = \int_{A_k} \left[[-\boldsymbol{D}_p]^T \hat{\boldsymbol{C}}_{\sigma_p\epsilon_p}^k \boldsymbol{D}_p \right] F_s F_\tau dz \,, \tag{32}$$

$$\boldsymbol{K}_{u\sigma}^{k\tau s} = \int_{A_k} \left[-\boldsymbol{D}_p]^T \hat{\boldsymbol{C}}_{\sigma_p\sigma_n}^k + [-\boldsymbol{D}_{n\Omega} + \boldsymbol{D}_{nz}]^T \right] F_s F_\tau dz \,, \tag{33}$$

$$\boldsymbol{K}_{\sigma u}^{k\tau s} = \int_{A_k} \left[[\boldsymbol{D}_{n\Omega} + \boldsymbol{D}_{nz}] - \hat{\boldsymbol{C}}_{\epsilon_n\epsilon_p}^k \boldsymbol{D}_p \right] F_s F_\tau dz \,, \tag{34}$$

$$\boldsymbol{K}_{\sigma\sigma}^{k\tau s} = \int_{A_k} \left[-\hat{\boldsymbol{C}}_{\epsilon_n\sigma_n}^k \right] F_s F_\tau dz \,, \tag{35}$$

and the nuclei for the boundary conditions are:

$$\boldsymbol{\Pi}_u^{k\tau s} = \int_{A_k} \left[\boldsymbol{I}_p^T \hat{\boldsymbol{C}}_{\sigma_p\epsilon_p}^k \boldsymbol{D}_p \right] F_s F_\tau dz \,, \tag{36}$$

$$\boldsymbol{\Pi}_\sigma^{k\tau s} = \int_{A_k} \left[\boldsymbol{I}_p^T \hat{\boldsymbol{C}}_{\sigma_p\sigma_n}^k + \boldsymbol{I}_{n\Omega}^T \right] F_s F_\tau dz \,, \tag{37}$$

The nuclei in the explicit form are:

$$
\begin{aligned}
K^{k\tau s}_{uu_{11}} =&(-\partial^\tau_x\partial^s_x C_{11} - \partial^\tau_x\partial^s_y C_{16} - \partial^\tau_y\partial^s_x C_{16} + \partial^\tau_x\partial^s_x\frac{C^2_{13}}{C_{33}} + \partial^\tau_x\partial^s_y\frac{C_{13}C_{36}}{C_{33}} + \\
&\partial^\tau_y\partial^s_x\frac{C_{13}C_{36}}{C_{33}} + \partial^\tau_y\partial^s_y\frac{C^2_{36}}{C_{33}} - \partial^\tau_y\partial^s_y C_{66})F_\tau F_s \\
K^{k\tau s}_{uu_{12}} =&(-\partial^\tau_x\partial^s_y C_{12} - \partial^\tau_x\partial^s_x C_{16} - \partial^\tau_y\partial^s_y C_{26} + \partial^\tau_x\partial^s_y\frac{C_{13}C_{23}}{C_{33}} + \partial^\tau_x\partial^s_x\frac{C_{13}C_{36}}{C_{33}} + \\
&\partial^\tau_y\partial^s_y\frac{C_{23}C_{36}}{C_{33}} + \partial^\tau_y\partial^s_x\frac{C^2_{36}}{C_{33}} - \partial^\tau_y\partial^s_x C_{66})F_\tau F_s \\
K^{k\tau s}_{uu_{13}} =&0 \\
K^{k\tau s}_{uu_{21}} =&(-\partial^\tau_y\partial^s_x C_{12} - \partial^\tau_x\partial^s_x C_{16} - \partial^\tau_y\partial^s_y C_{26} + \partial^\tau_y\partial^s_x\frac{C_{13}C_{23}}{C_{33}} + \partial^\tau_x\partial^s_x\frac{C_{13}C_{36}}{C_{33}} + \\
&\partial^\tau_y\partial^s_y\frac{C_{23}C_{36}}{C_{33}} + \partial^\tau_x\partial^s_y\frac{C^2_{36}}{C_{33}} - \partial^\tau_x\partial^s_y C_{66})F_\tau F_s \\
K^{k\tau s}_{uu_{22}} =&(-\partial^\tau_y\partial^s_y C_{22} - \partial^\tau_x\partial^s_y C_{26} - \partial^\tau_y\partial^s_x C_{26} + \partial^\tau_y\partial^s_y\frac{C^2_{23}}{C_{33}} + \partial^\tau_x\partial^s_y\frac{C_{23}C_{36}}{C_{33}} + \\
&\partial^\tau_y\partial^s_x\frac{C_{23}C_{36}}{C_{33}} + \partial^\tau_x\partial^s_x\frac{C^2_{36}}{C_{33}} - \partial^\tau_x\partial^s_x C_{66})F_\tau F_s \\
K^{k\tau s}_{uu_{23}} =&K^{k\tau s}_{uu_{31}} = K^{k\tau s}_{uu_{32}} = K^{k\tau s}_{uu_{33}} = 0
\end{aligned}
\tag{38}
$$

$$
\begin{aligned}
&K^{k\tau s}_{u\sigma_{11}} = \partial^\tau_z F_\tau F_s, \quad K^{k\tau s}_{u\sigma_{12}} = 0; \quad K^{k\tau s}_{u\sigma_{13}} = (-\partial^\tau_x\frac{C_{13}}{C_{33}} - \partial^\tau_y\frac{C_{36}}{C_{33}})F_\tau F_s \\
&K^{k\tau s}_{u\sigma_{21}} = 0; \quad K^{k\tau s}_{u\sigma_{22}} = \partial^\tau_z F_\tau F_s; \quad K^{k\tau s}_{u\sigma_{23}} = (-\partial^\tau_y\frac{C_{23}}{C_{33}} - \partial^\tau_x\frac{C_{36}}{C_{33}})F_\tau F_s \\
&K^{k\tau s}_{u\sigma_{31}} = -\partial^\tau_x F_\tau F_s; \quad K^{k\tau s}_{u\sigma_{32}} = -\partial^\tau_y F_\tau F_s; \quad K^{k\tau s}_{u\sigma_{33}} = \partial^\tau_z F_\tau F_s
\end{aligned}
\tag{39}
$$

$$
\begin{aligned}
K^{k\tau s}_{\sigma u_{11}} =&\partial^s_z F_\tau F_s; \quad K^{k\tau s}_{\sigma u_{12}} = 0; \quad K^{k\tau s}_{\sigma u_{13}} = \partial^s_x F_\tau F_s \\
K^{k\tau s}_{\sigma u_{21}} =&0; \quad K^{k\tau s}_{\sigma u_{22}} = \partial^s_z F_\tau F_s; \quad K^{k\tau s}_{\sigma u_{23}} = \partial^s_y F_\tau F_s \\
K^{k\tau s}_{\sigma u_{31}} =&(\partial^s_x\frac{C_{13}}{C_{33}} + \partial^s_y\frac{C_{36}}{C_{33}})F_\tau F_s; \quad K^{k\tau s}_{\sigma u_{32}} = (\partial^s_y\frac{C_{23}}{C_{33}} + \partial^s_x\frac{C_{36}}{C_{33}})F_\tau F_s; \quad K^{k\tau s}_{\sigma u_{33}} = \partial^s_z F_\tau F_s
\end{aligned}
\tag{40}
$$

$$
\begin{aligned}
K^{k\tau s}_{\sigma\sigma_{11}} &= \frac{C_{44}}{C_{45}^2 - C_{44}C_{55}} F_\tau F_s; \quad K^{k\tau s}_{\sigma\sigma_{12}} = \frac{C_{45}}{-C_{45}^2 + C_{44}C_{55}} F_\tau F_s; \quad K^{k\tau s}_{\sigma\sigma_{13}} = 0 \\
K^{k\tau s}_{\sigma\sigma_{21}} &= \frac{C_{45}}{-C_{45}^2 + C_{44}C_{55}} F_\tau F_s; \quad K^{k\tau s}_{\sigma\sigma_{22}} = \frac{C_{55}}{C_{45}^2 - C_{44}C_{55}} F_\tau F_s; \quad K^{k\tau s}_{\sigma\sigma_{23}} = 0 \\
K^{k\tau s}_{\sigma\sigma_{31}} &= 0; \quad K^{k\tau s}_{\sigma\sigma_{32}} = 0; \quad K^{k\tau s}_{\sigma\sigma_{33}} = -\frac{1}{C_{33}} F_\tau F_s
\end{aligned} \tag{41}
$$

$$
\begin{aligned}
\Pi^{k\tau s}_{u_{11}} =& (n_x\partial_x^s C_{11} + n_x\partial_y^s C_{16} + n_y\partial_x^s C_{16} - n_x\partial_x^s \frac{C_{13}^2}{C_{33}} - n_x\partial_y^s \frac{C_{13}C_{36}}{C_{33}} - \\
& n_y\partial_x^s \frac{C_{13}C_{36}}{C_{33}} - n_y\partial_y^s \frac{C_{36}^2}{C_{33}} + n_y\partial_y^s C_{66}) F_\tau F_s \\
\Pi^{k\tau s}_{u_{12}} =& (n_x\partial_y^s C_{12} + n_x\partial_x^s C_{16} + n_y\partial_y^s C_{26} - n_x\partial_y^s \frac{C_{13}C_{23}}{C_{33}} - n_x\partial_x^s \frac{C_{13}C_{36}}{C_{33}} - \\
& n_y\partial_y^s \frac{C_{23}C_{36}}{C_{33}} - n_y\partial_x^s \frac{C_{36}^2}{C_{33}} + n_y\partial_x^s C_{66}) F_\tau F_s \\
\Pi^{k\tau s}_{u_{13}} =& 0 \\
\Pi^{k\tau s}_{u_{21}} =& (n_y\partial_x^s C_{12} + n_x\partial_x^s C_{16} + n_y\partial_y^s C_{26} - n_y\partial_x^s \frac{C_{13}C_{23}}{C_{33}} - n_x\partial_x^s \frac{C_{13}C_{36}}{C_{33}} - \\
& n_y\partial_y^s \frac{C_{23}C_{36}}{C_{33}} - n_x\partial_y^s \frac{C_{36}^2}{C_{33}} + n_x\partial_y^s C_{66}) F_\tau F_s \\
\Pi^{k\tau s}_{u_{22}} =& (n_y\partial_y^s C_{22} + n_x\partial_y^s C_{26} + n_y\partial_x^s C_{26} - n_y\partial_y^s \frac{C_{23}^2}{C_{33}} - n_x\partial_y^s \frac{C_{23}C_{36}}{C_{33}} - \\
& n_y\partial_x^s \frac{C_{23}C_{36}}{C_{33}} - n_x\partial_x^s \frac{C_{36}^2}{C_{33}} + n_x\partial_x^s C_{66}) F_\tau F_s \\
\Pi^{k\tau s}_{u_{23}} =& \Pi^{k\tau s}_{u_{31}} = \Pi^{k\tau s}_{u_{32}} = \Pi^{k\tau s}_{u_{33}} = 0
\end{aligned} \tag{42}
$$

$$
\begin{aligned}
\Pi^{k\tau s}_{\sigma_{11}} &= 0; \quad \Pi^{k\tau s}_{\sigma_{12}} = 0; \quad \Pi^{k\tau s}_{\sigma_{13}} = (n_x \frac{C_{13}}{C_{33}} + n_y \frac{C_{36}}{C_{33}}) F_\tau F_s \\
\Pi^{k\tau s}_{\sigma_{21}} &= 0; \quad \Pi^{k\tau s}_{\sigma_{22}} = 0; \quad \Pi^{k\tau s}_{\sigma_{23}} = (n_y \frac{C_{23}}{C_{33}} + n_x \frac{C_{36}}{C_{33}}) F_\tau F_s \\
\Pi^{k\tau s}_{\sigma_{31}} &= n_x F_\tau F_s; \quad \Pi^{k\tau s}_{\sigma_{32}} = n_y F_\tau F_s; \quad \Pi^{k\tau s}_{\sigma_{33}} = 0
\end{aligned} \tag{43}
$$

The dynamic problem is expressed as:

$$\sum_{k=1}^{N_l} \int_{\Omega_k} \int_{A_k} \left\{ \delta {\epsilon_{pG}^k}^T \sigma_{pC}^k + \delta {\epsilon_{nG}^k}^T \sigma_{nC}^k \right\} d\Omega_k dz = \sum_{k=1}^{N_l} \int_{\Omega_k} \int_{A_k} \rho^k \delta \mathbf{u}^{kT} \ddot{\mathbf{u}}^k d\Omega_k dz + \sum_{k=1}^{N_l} \delta L_e^k \tag{44}$$

where ρ^k is the mass density of the k-th layer and double dots denote acceleration.

By substituting the geometrical relations, the constitutive equations and the Unified Formulation, we obtain the following governing equations:

$$\delta {\mathbf{u}_s^k}^T \; : \qquad \mathbf{K}_{uu}^{k\tau s} \, \mathbf{u}_\tau^k = \mathbf{M}^{k\tau s} \ddot{\mathbf{u}}_\tau^k + \mathbf{P}_{u\tau}^k \tag{45}$$

In the case of free vibrations one has:

$$\delta {\mathbf{u}_s^k}^T \; : \qquad \mathbf{K}_{uu}^{k\tau s} \, \mathbf{u}_\tau^k = \mathbf{M}^{k\tau s} \ddot{\mathbf{u}}_\tau^k \tag{46}$$

where $\mathbf{M}^{k\tau s}$ is the fundamental nucleus for the inertial term. The explicit form of that is:

$$M_{11}^{k\tau s} = \rho^k F_\tau F_s; \qquad M_{12}^{k\tau s} = 0; \quad M_{13}^{k\tau s} = 0 \tag{47}$$

$$M_{21}^{k\tau s} = 0; \qquad M_{22}^{k\tau s} = \rho^k F_\tau F_s; \quad M_{23}^{k\tau s} = 0 \tag{48}$$

$$M_{31}^{k\tau s} = 0; \qquad M_{32}^{k\tau s} = 0; \quad M_{33}^{k\tau s} = \rho^k F_\tau F_s \tag{49}$$

At this point, we would like to note that the same radial basis functions are used for the interpolation of all the unknowns, displacements and stresses alike.

4 Numerical examples

All numerical examples consider a Chebyshev grid and a Wendland function, defined as

$$\phi(r) = (1 - c\, r)_+^8 \left(32(c\, r)^3 + 25(c\, r)^2 + 8c\, r + 1 \right) \tag{50}$$

where the shape parameter (c) was obtained by an optimization procedure, as in Ferreira and Fasshauer [45].

4.1 Static problems-cross-ply laminated plates

A simply supported square laminated plate of side a and thickness h is composed of four equally layers oriented at $[0°/90°/90°/0°]$. The plate is subjected to a sinusoidal vertical pressure of the form

$$p_z = P \sin\left(\frac{\pi x}{a}\right) \sin\left(\frac{\pi y}{a}\right)$$

with the origin of the coordinate system located at the lower left corner on the midplane and P the maximum load (note the load is applied on top of the plate).

The orthotropic material properties for each layer are given by

$$E_1 = 25.0E_2 \qquad G_{12} = G_{13} = 0.5E_2 \qquad G_{23} = 0.2E_2 \qquad \nu_{12} = 0.25$$

The degrees of freedom for a 4-layered laminate are ilustrated in figure 1. For this case the total number of degrees of freedom are $(30 \times N)$, where N is the total number of discretization points.

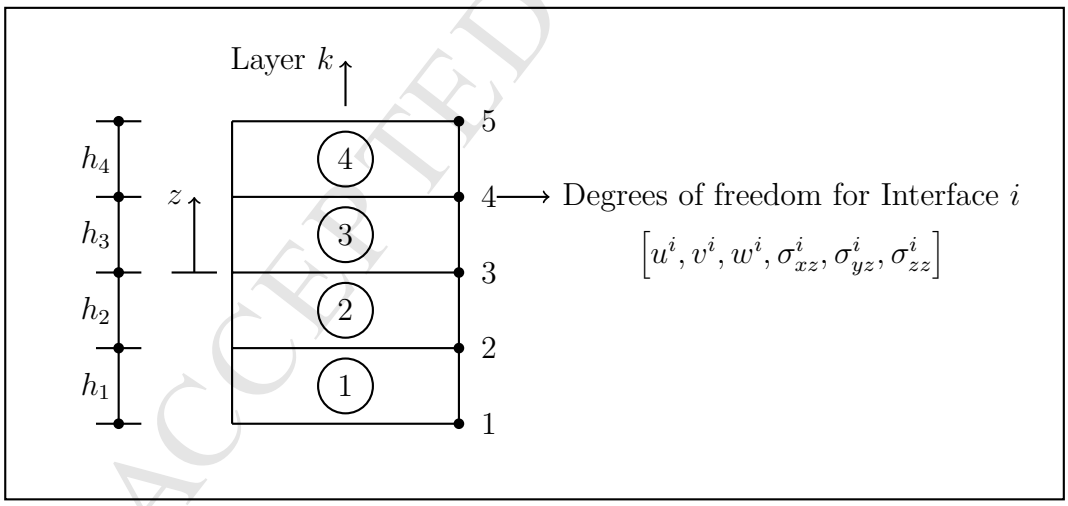

Fig. 1. A 4-layer laminate; definition of degrees of freedom at interfaces

The in-plane displacements, the transverse displacements, the normal stresses and the in-plane and transverse shear stresses are presented in normalized form as

$$w = \frac{10^2 w_{(a/2,a/2,0)} h^3 E_2}{P a^4} \qquad \sigma_{xx} = \frac{\sigma_{xx(a/2,a/2,h/2)} h^2}{P a^2} \qquad \sigma_{yy} = \frac{\sigma_{yy(a/2,a/2,h/4)} h^2}{P a^2}$$

$$\tau_{xz} = \frac{\tau_{xz(0,a/2,0)} h}{P a}$$

In table 1 we present results for the present RMVT approach, using 13×13 up to 21×21 points. We compare results with higher-order solutions by Reddy [46], FSDT solutions by Reddy and Chao [47], and an exact solution by Pagano [1]. The present RMVT meshless approach produces excellent results, when compared with the exact solutions, for all a/h ratios, for transverse displacements, normal stresses and transverse shear stresses. It is clear that the FSDT cannot be used for thick laminates. In figure 2 the σ_{xx} evolution across the thickness direction is illustrated, for $a/h = 4$, using 21×21 points. In figure 3 the τ_{xz} evolution across the thickness direction is illustrated, for $a/h = 4$, using 21×21 points. Note that the transverse shear stresses are obtained directly at each interface directly from the constitutive equations.

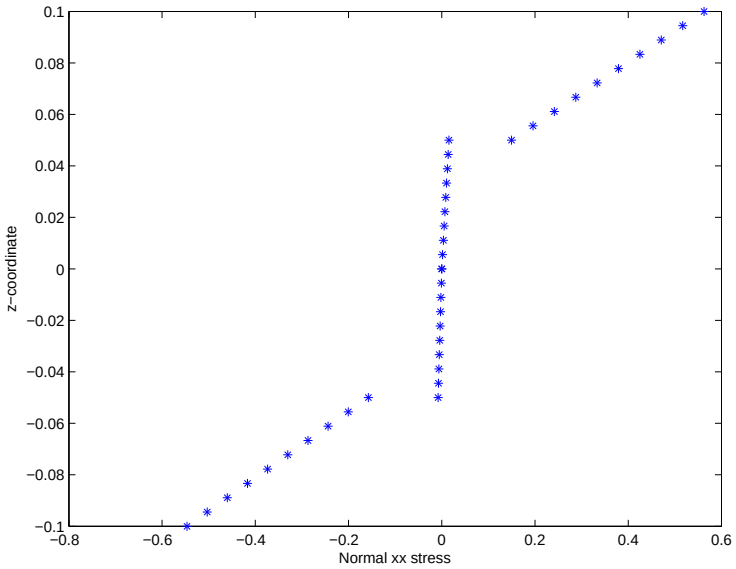

Fig. 2. Normalized normal σ_{xx} stress for $a/h = 4$, 21×21 points

4.2 Sandwich plate

In this example, we consider a simply-supported square sandwich plate loaded by uniform transverse pressure p. The length and thickness of the plate are

$\frac{a}{h}$	Method	w	σ_{xx}	σ_{yy}	τ_{zx}
4	HSDT [46]	1.8937	0.6651	0.6322	0.2064
	FSDT [47]	1.7100	0.4059	0.5765	0.1398
	elasticity [1]	1.954	0.720	0.666	0.270
	present (13×13 grid)	1.9784	0.6766	0.5872	0.2332
	present (17×17 grid)	1.9783	0.6766	0.5872	0.2332
	present (21×21 grid)	1.9783	0.6765	0.5872	0.2332
10	HSDT [46]	0.7147	0.5456	0.3888	0.2640
	FSDT [47]	0.6628	0.4989	0.3615	0.1667
	elasticity [1]	0.743	0.559	0.403	0.301
	present (13×13 grid)	0.7326	0.5627	0.3909	0.3321
	present (17×17 grid)	0.7325	0.5627	0.3908	0.3321
	present (21×21 grid)	0.7325	0.5627	0.3908	0.3321
100	HSDT [46]	0.4343	0.5387	0.2708	0.2897
	FSDT [47]	0.4337	0.5382	0.2705	0.1780
	elasticity [1]	0.4347	0.539	0.271	0.339
	present (13×13 grid)	0.4308	0.5432	0.2731	0.3774
	present (17×17 grid)	0.4307	0.5431	0.2730	0.3771
	present (21×21 grid)	0.4307	0.5431	0.2730	0.3768

Table 1
$[0°/90°/90°/0°]$ square laminated plate under two higher-order Zig-Zag formulations

denoted by a, h, respectively. The plate ratio a/h is taken as 10. It consists of a two skins with equal thickness $(0.1h)$ with the following mechanical properties:

$$E_1/E_2 = 25; \quad G_{12}/E_2 = G_{13}/E_2 = 0.5; \quad G_{23}/E_2 = 0.2; \quad \nu_{12} = 0.25 \quad (51)$$

while the inner layer, the weak core, has a thickness of $0.8h$ and the following mechanical properties:

$$E_1/E_2 = 1; \quad G_{13}/E_2 = G_{23}/E_2 = 0.06; \quad G_{12}/E_2 = 0.016; \quad \nu_{12} = 0.25 \quad (52)$$

In Table 2 the present RBF formulation is compared with closed-form results by Carrera and Ciuffreda [48]. Depending on the used variational statement (PVD or RMVT), the description of the variables (LWM or ESLM), the order of the used expansion N, a number of two-dimensional theories can be constructed. In order to denote different theories in a concise manner, acronims

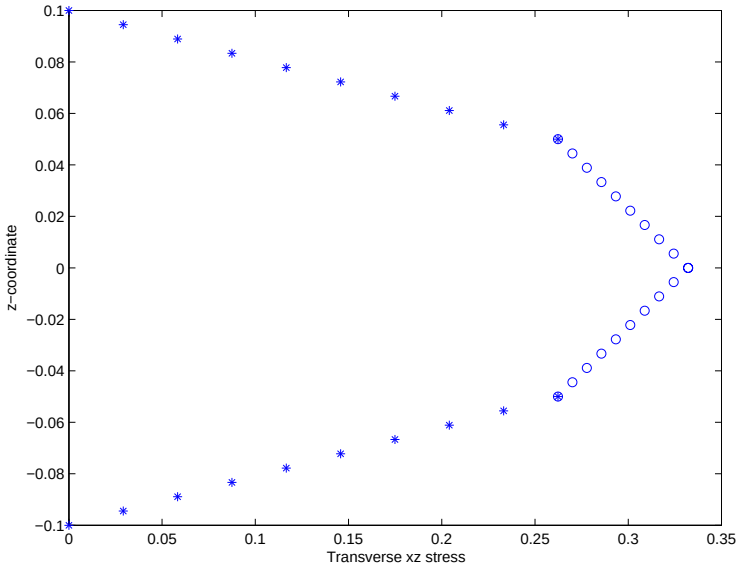

Fig. 3. Normalized transverse τ_{xz} stress for $a/h = 4$, 21×21 points

could conveniently used. Transverse stress and displacement z-fields have the assumptions for layer-wise mixed cases: LM1(Layer-wise Mixed, linear) and LM4 (Layer-wise Mixed, fourth-order). Only displacement assumptions are made for LD1 (Layer-wise Displacement, linear) and LD3 (Layer-wise Displacement, cubic) cases. A parabolic transverse stress field in each-layer is associated to linear a zig-zag diplacement field for the EMZC1 case (Equivalent-single-layer Mixed including Zig-zag and interlaminar-Continuity, linear) and fourth-order transverse stress field in each-layer is associated to a cubic zig-zag displacement field for the EMZC3 case (Equivalent-single-layer Mixed including Zig-zag and interlaminar-Continuity, cubic). The EMZC3d approach is related with a theory that accounts for constant W across the thickness direction ($w = w_0$). The ED4 and ED1 are Equivalent-single-layer displacement-based theories of the fourth-order and first-order types. .

Results are presented for transverse displacements $U_z(a/2, b/2, 0)$, and in-plane $S_{xx}(a/2, b/2, h/2)$ and out-of-plane stress $S_{xz}(0, b/2, 0)$. Figure 4 illustrate the evolution of the normal stress S_{xx} across the thickness direction, for $a/h = 4$. Figure 5 illustrate the evolution of the transverse shear stress S_{xz} across the thickness direction, for $a/h = 4$.

4.3 Free vibration problems-cross-ply laminated plates

In this example, all layers of the laminate are assumed to be of the same thickness, density and made of the same linearly elastic composite material.

	U_z			S_{xx}			S_{xz}		
a/h	4	10	100	4	10	100	4	10	100
11×11	10.7186	3.1110	1.2671	1.9322	1.5389	1.5188	0.3981	0.5217	0.5476
13×13	10.6774	3.1013	1.2656	1.9024	1.5293	1.5184	0.3984	0.5243	0.5849
17×17	10.6708	3.0983	1.2650	1.8897	1.5191	1.5177	0.3994	0.5220	0.5984
LM4	10.682	3.083	1.262	1.902	1.509	1.505	0.4074	0.5276	0.5889
EMZC3	10.678	3.082	1.262	1.899	1.507	1.504	0.3949	0.5239	0.5886
EMZC3d	10.626	3.026	1.230	1.915	1.480	1.476	0.4031	0.5224	0.5865
ED4	9.909	2.923	1.260	1.929	1.519	1.506	0.3574	0.5104	0.5881
ED1	5.542	1.982	1.218	1.145	1.388	1.475	0.5249	0.5716	0.5876
FSDT	5.636	1.984	1.218	1.168	1.391	1.476	0.5249	0.5716	0.5876
CLT	1.2103	1.2103	1.2103	1.476	1.476	1.476	0.5878	0.5878	0.5878

Table 2
Load applied at $z = h/2$: square sandwich plates

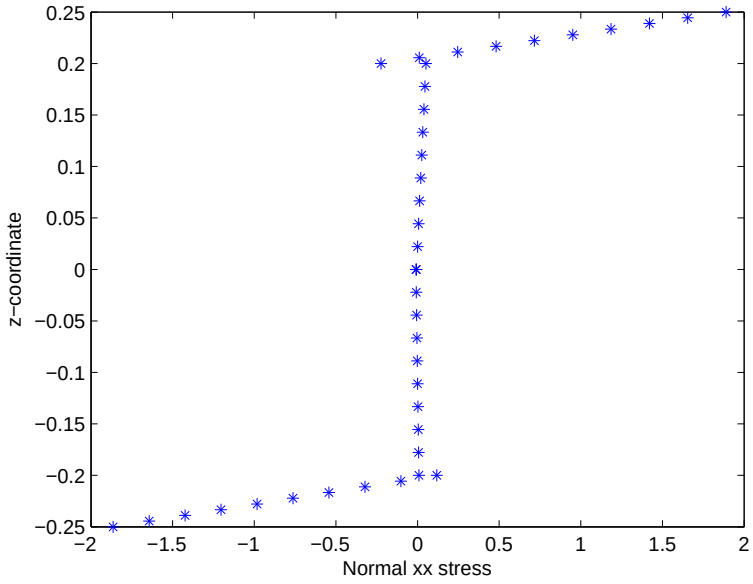

Fig. 4. Normalized normal S_{xx} stress for $a/h = 4$, 21×21 points, load at $z = h/2$

The following material parameters of a layer are used:

$$\frac{E_1}{E_2} = 10, 20, 30 \text{ or } 40; G_{12} = G_{13} = 0.6E_2; G_3 = 0.5E_2; \nu_{12} = 0.25$$

The subscripts 1 and 2 denote the directions normal and transverse to the

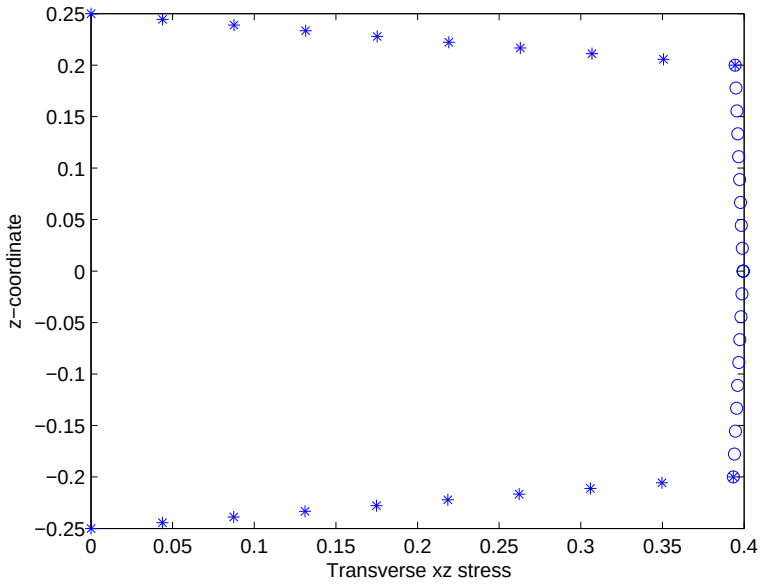

Fig. 5. Normalized transverse S_{xz} stress for $a/h = 4$, 21×21 points, load at $z = h/2$

fiber direction in a lamina, which may be oriented at an angle to the plate axes. The ply angle of each layer is measured from the global x-axis to the fiber direction.

The example considered is a simply supported square plate of the cross-ply lamination $[0°/90°/90°/0°]$. The thickness and length of the plate are denoted by h and a, respectively. The thickness-to-span ratio $h/a = 0.2$ is employed in the computation. Table 3 lists the fundamental frequency of the simply supported laminate made of various modulus ratios of E_1/E_2. Figure 6 illustrates the modes of vibration for $E_1/E_2 = 40$, grid 13×13 points. It is found that the present meshless results are in very close agreement with the values of [49] and the meshfree results of Liew [50] based on the FSDT. The small differences may be due to the consideration of the through-the-thickness deformations in the present formulation.

5 Conclusions

In this paper, we combined the Carrera's Unified Formulation and a radial basis function (RBF) collocation technique for predicting the static deformations and free vibrations behavior of thin and thick cross-ply laminated plates. For the first time, the Reissner-Mixed Variational Theorem was combined with the RBF collocation to achieve excelent results in terms of transverse displacements, direct transverse stresses at each layer interface, and free vibrations. This combination of methods has not been done before and serves to fill the

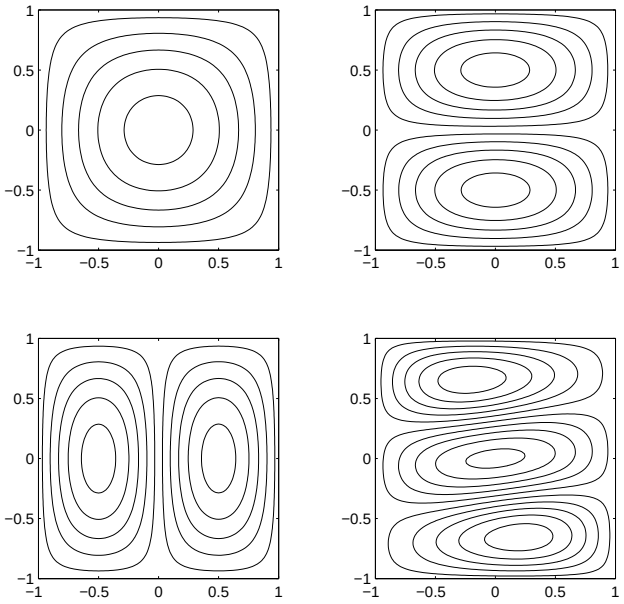

Fig. 6. First 4 modes of vibration of four-layer $[0°/90°/90°/0°]$ simply supported laminated plate $(\bar{w} = (wa^2/h)\sqrt{\rho/E_2}, h/a = 0.2), E_1/E_2 = 40$, grid 13×13 points

gap of knowledge in this area of research.

References

[1] N. J. Pagano. Exact solutions for rectangular bidirectional composites and sandwich plates. *Journal of Composite Materials*, 4:20–34, 1970.

[2] J. M. Whitney. The effect of transverse shear deformation in the bending of laminated plates. *J. Composite Materials*, 3:534–547, 1969.

[3] J. M. Whitney and A. W. Leissa. Analysis of heterogeneous anisotropic plates. *J. Appl. Mechanics*, 36(2):261–266, 1969.

[4] S. S. Vel and R. C. Batra. Three-dimensional exact solution for the vibration of functionally graded rectangular plates. *Journal of Sound and Vibration*, 272:703–730, 2004.

[5] R. C. Batra and S. Vidoli. Higher order piezoelectric plate theory derived from a three-dimensional variational principle. *AIAA Journal*, 40:91–104, 2002.

[6] E. Carrera and B. Kroplin. Zig-zag and interlaminar equilibria effects in large deflection and post-buckling analysis of multilayered plates. *Mechanics of Composite Materials and Structures*, 4:69–94, 1997.

[7] E. Carrera. Evaluation of layer-wise mixed theories for laminated plate analysis. *AIAA Journal*, (36):830–839, 1998.

[8] E. Carrera. Developments, ideas, and evaluations based upon reissner's mixed variational theorem in the modelling of multilayered plates and shells. *Applied Mechanics Reviews*, 54:301–329, 2001.

[9] E. Carrera. C^0 reissner-mindlin multilayered plate elements including zig-zag and interlaminar stress continuity. *International Journal of Numerical Methods in Engineering*, 39:1797–1820, 1996.

[10] A. J. M. Ferreira, C. M. C. Roque, E. Carrera, and M. Cinefra. Analysis of laminated doubly-curved shells by a layerwise theory and radial basis functions collocation, accounting for through-the-thickness deformations. *Computational Mechanics*, 48:13–25, 2011.

[11] A. J. M. Ferreira, C. M. C. Roque, E. Carrera, M. Cinefra, and O. Polit. Analysis of laminated shells by a sinusoidal shear deformation theory and radial basis functions collocation, accounting for through-the-thickness deformations. *Composites: Part B*, 42:1276–1284, 2011.

[12] A. J. M. Ferreira, C. M. C. Roque, E. Carrera, M. Cinefra, and O. Polit. Two higher-order zig-zag theories for accurate bending, vibration and buckling response of laminated plates by radial basis functions collocation and a unified formulation. *Journal of Composite Materials*, 45:2523–2536, 2011.

[13] A. J. M. Ferreira, C. M. C. Roque, E. Carrera, M. Cinefra, and O. Polit. A refinement of murakami's zig-zag theory for bending, vibration and buckling analysis of laminated plates by radial basis functions and a unified formulation. *European Journal of Mechanics, A/Solids*, 30:559–570, 2011.

[14] A. J. M. Ferreira, C. M. C. Roque, E. Carrera, and M. Cinefra. Analysis of thick isotropic and cross-ply laminated plates by radial basis functions and unified formulation. *Journal of Sound and Vibration*, 330:771–787, 2011.

[15] Y. C. Hon, M. W. Lu, W. M. Xue, and Y. M. Zhu. Multiquadric method for the numerical solution of byphasic mixture model. *Applied Mathematics and Computation*, 88:153–175, 1997.

[16] Y. C. Hon, K. F. Cheung, X. Z. Mao, and E. J. Kansa. A multiquadric solution for the shallow water equation. *ASCE Journal of Hydraulic Engineering*, 125(5):524–533, 1999.

[17] J. G. Wang, G. R. Liu, and P. Lin. Numerical analysis of biot's consolidation process by radial point interpolation method. *International Journal of Solids and Structures*, 39(6):1557–1573, 2002.

[18] G. R. Liu and Y. T. Gu. A local radial point interpolation method (lrpim) for free vibration analyses of 2-d solids. *Journal of Sound and Vibration*, 246(1):29–46, 2001.

[19] G. R. Liu and J. G. Wang. A point interpolation meshless method based on radial basis functions. *International Journal for Numerical Methods in Engineering*, 54:1623–1648, 2002.

[20] J. G. Wang and G. R. Liu. On the optimal shape parameters of radial basis functions used for 2-d meshless methods. *Computer Methods in Applied Mechanics and Engineering*, 191:2611–2630, 2002.

[21] X. L. Chen, G. R. Liu, and S. P. Lim. An element free galerkin method for the free vibration analysis of composite laminates of complicated shape. *Composite Structures*, 59:279–289, 2003.

[22] K. Y. Dai, G. R. Liu, S. P. Lim, and X. L. Chen. An element free galerkin method for static and free vibration analysis of shear-deformable laminated composite plates. *Journal of Sound and Vibration*, 269:633–652, 2004.

[23] G. R. Liu and X. L. Chen. Buckling of symmetrically laminated composite plates using the element-free galerkin method. *International Journal of Structural Stability and Dynamics*, 2:281–294, 2002.

[24] K. M. Liew, X. L. Chen, and J. N. Reddy. Mesh-free radial basis function method for buckling analysis of non-uniformity loaded arbitrarily shaped shear deformable plates. *Computer Methods in Applied Mechanics and Engineering*, 193:205–225, 2004.

[25] Y. Q Huang and Q. S. Li. Bending and buckling analysis of antisymmetric laminates using the moving least square differential quadrature method. *Computer Methods in Applied Mechanics and Engineering*, 193:3471–3492, 2004.

[26] L. Liu, G. R. Liu, and V. C. B. Tan. Element free method for static and free vibration analysis of spatial thin shell structures. *Computer Methods in Applied Mechanics and Engineering*, 191:5923–5942, 2002.

[27] S. Xiang, K. M. Wang, Y. T. Ai, Y. D. Sha, and H. Shi. Analysis of isotropic, sandwich and laminated plates by a meshless method and various shear deformation theories. *Composite Structures*, 91(1):31–37, 2009.

[28] S. Xiang, H. Shi, K. M. Wang, Y. T. Ai, and Y. D. Sha. Thin plate spline radial basis functions for vibration analysis of clamped laminated composite plates. *European Journal of Mechanics A/Solids*, 29:844–850, 2010.

[29] T. Rabczuk and P. Areias. A meshfree thin shell for arbitrary evolving cracks based on an extrinsic basis. *CMES - Computer Modeling in Engineering and Sciences*, 16(2):115–130, 2006.

[30] T. Rabczuk, P.M.A. Areias, and T. Belytschko. A meshfree thin shell method for non-linear dynamic fracture. *International Journal for Numerical Methods in Engineering*, 72(5):524–548, 2007.

[31] N. Nguyen-Thanh, T. Rabczuk, H. Nguyen-Xuan, and S. Bordas. An alternative alpha finite element method with discrete shear gap technique for analysis of isotropic mindlin-reissner plates. *Finite Elements in Analysis and Design*, 47(5):519–535, 2011.

[32] C. Thai-Hoang, N. Nguyen-Thanh, H. Nguyen-Xuan, and T. Rabczuk. An alternative alpha finite element method with discrete shear gap technique for analysis of laminated composite plates. *Applied Mathematics and Computation*, 217(17):7324–7348, 2011.

[33] E. J. Kansa. Multiquadrics- a scattered data approximation scheme with applications to computational fluid dynamics. i: Surface approximations and partial derivative estimates. *Computers and Mathematics with Applications*, 19(8/9):127–145, 1990.

[34] A. J. M. Ferreira. A formulation of the multiquadric radial basis function method for the analysis of laminated composite plates. *Composite Structures*, 59:385–392, 2003.

[35] A. J. M. Ferreira. Thick composite beam analysis using a global meshless approximation based on radial basis functions. *Mechanics of Advanced Materials and Structures*, 10:271–284, 2003.

[36] A. J. M. Ferreira, C. M. C. Roque, and P. A. L. S. Martins. Analysis of composite plates using higher-order shear deformation theory and a finite point formulation based on the multiquadric radial basis function method. *Composites: Part B*, 34:627–636, 2003.

[37] E. Carrera. Historical review of zig-zag theories for multilayered plates and shells. *Applied Mechanics Reviews*, (56):287–308, 2003.

[38] R. D. Mindlin. Influence of rotary inertia and shear in flexural motions of isotropic elastic plates. *Journal of Applied mechanics*, 18:31–38, 1951.

[39] P. C. Yang, C. H. Norris, and Y. Stavsky. Elastic wave propagation in heterogeneous plates. *International Journal of Solids and Structures*, 2:665–684, 1966.

[40] J. N. Reddy. Bending of laminated anisotropic shells by a shear deformable finite element. *Fibre Science and Technology*, 17(1):9–24, 1982.

[41] J. N. Reddy. *Mechanics of laminated composite plates*. CRC Press, New York, 1997.

[42] B. N. Pandya and T. Kant. Higher-order shear deformable theories for flexure of sandwich plates-finite element evaluations. *International Journal of Solids and Structures*, 24:419–451, 1988.

[43] C. T. Sun. Theory of laminated plates. *Journal of Applied Mechanics*, 38:231–238, 1971.

[44] J. M. Whitney and C. T. Sun. A refined theory for laminated anisotropic cylindrical shells. *Journal of Applied Mechanics*, 41, 1974.

[45] A. J. M. Ferreira and G. E. Fasshauer. Computation of natural frequencies of shear deformable beams and plates by a rbf-pseudospectral method. *Computer Methods in Applied Mechanics and Engineering*, 196:134–146, 2006.

[46] J. N. Reddy. A simple higher-order theory for laminated composite plates. *Journal of Applied Mechanics*, 51:745–752, 1984.

[47] J. N. Reddy and W. C. Chao. A comparison of closed-form and finite-element solutions of thick laminated anisotropic rectangular plates. *Nuclear Engineering and Design*, 64:153–167, 1981.

[48] E. Carrera and A. Ciuffreda. A unified formulation to assess theories of multilayered plates for various bending problems. *Compos. Struct.*, 69:4271–293, 2005.

[49] A. A. Khdeir and L. Librescu. Analysis of symmetric cross-ply elastic plates using a higher-order theory,part ii: buckling and free vibration. *Composite Structures*, 9:259–277, 1988.

[50] K. M. Liew, Y. Q. Huang, and J. N. Reddy. Vibration analysis of symmetrically laminated plates based on fsdt using the moving least squares differential quadrature method. *Computer Methods in Applied Mechanics and Engineering*, 192:2203–2222, 2003.

Method	Grid	E_1/E_2			
		10	20	30	40
Liew [50]		8.2924	9.5613	10.320	10.849
Exact (Reddy, Khdeir)[49]		8.2982	9.5671	10.326	10.854
Present ($\nu_{23} = 0.49$)	11×11	8.2866	9.5391	10.2676	10.7590
	13×13	8.2863	9.5388	10.2673	10.8035
	17×17	8.2862	9.5387	10.2672	10.8034

Table 3
The normalized fundamental frequency of the simply-supported cross-ply laminated square plate $[0°/90°/90°/0°]$ ($\bar{w} = (wa^2/h)\sqrt{\rho/E_2}, h/a = 0.2$)